

Numerical Simulation and Its Possibility of Application to Green Environment

Anna Kuwana ^{1,a}, Tetuya Kawamura ^{2,b}

¹ Faculty of Science and Technology, Gunma University, 1-5-1 Tenjin-cho, Kiryu City, Gunma
376-8515, Japan

²Graduate School of Humanities and Sciences, Ochanomizu University, 2-1-1 Ohtsuka, Bunkyo-ku,
Tokyo 112-8610, Japan

^a<kuwana.anna@gunma-u.ac.jp>, ^b<kawamura@is.ocha.ac.jp>

Keywords: numerical simulation, green environment, visualization.

Abstract. Computers have advanced very much in recent years. Thanks to that, numerical simulation has become useful as a third research method that is just like theory and experiment. Numerical simulation is carried out with following steps: Express the physical law which governs the phenomenon by mathematical expression. Make numerical model so that computer can calculate them. Huge numerical calculations are carried out by using computer's computing power. Visualize numerical data. If the equations governing the phenomena are obtained, various problems could be simulated. As one example of numerical simulation related to green environment, wind turbine will be reported in this paper. Fluid motion around a wind turbine and torque which rotates the turbine are calculated. The wind turbine in the stationary state is pushed by the wind and it started rotating. The rotation speed of the wind turbine corresponding to the angle of the wind turbine could be calculated. It permits to simulate under more realistic conditions.

1. Introduction

The numerical simulation mentioned here is a simulated experiment executed on a computer. Numerical simulation has become useful as a third research method that is just like theory and experiment. It can be a powerful research method for topics where experiments and observations are difficult. For example, very large things like planets, very small things like microorganism, complex problem, expensive things, the time scale of things are very short, the topic which is required very long observation time like change in terrain.

A rotational mechanism to obtain natural energy called "wind turbine" will be reported in this paper, as one example of numerical simulation related to green environment. It is noteworthy that vertical-axis wind turbines powered by drag of wind can rotate stably with weak wind.

2. A Wind Turbine Mentioned in This Paper

A Savonius rotor is shown in Fig.1. It is consisted from two half cylinders [1]. The Savonius rotor rotates by the force pushing the blade called "drag". Unlike a wind turbine that rotates with lift, Savonius rotor cannot rotate at high speed, but it can start to rotate also without strong wind. Therefore, it works well in urban areas where wind strength and direction are not stable. It is characterized by overlap of blades. The passing wind between the blades helps the rotation. The shape of the blade of rotor determines power generation efficiency [2].

In many cases, the basic characteristics are measured with a wind turbine rotated at a constant angular velocity that unrelated with real

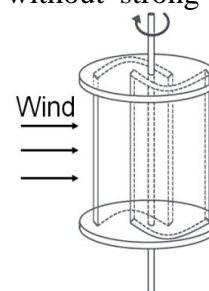


Fig. 1. Savonius rotor.

wind. Numerical simulation was carried out for time-varying rotation in this paper.

3. Numerical Method

3.1 Basic Equations of Fluid

The flow around the Savonius rotor is governed by the incompressible Navier-Stokes equations. A two-dimensional plane considered as the cross section of the rotor is calculated in this paper. Basic equations fixed on the rotating blade are as follows:

Continuity:

$$\frac{\partial U}{\partial X} + \frac{\partial V}{\partial Y} = 0 \quad (1)$$

Motion:

$$\frac{\partial U}{\partial t} + U \frac{\partial U}{\partial X} + V \frac{\partial U}{\partial Y} - \omega^2 X + 2\omega V = -\frac{\partial p}{\partial X} + \frac{1}{\text{Re}} \left(\frac{\partial^2 U}{\partial X^2} + \frac{\partial^2 U}{\partial Y^2} \right) \quad (2)$$

$$\frac{\partial V}{\partial t} + U \frac{\partial V}{\partial X} + V \frac{\partial V}{\partial Y} - \omega^2 Y - 2\omega U = -\frac{\partial p}{\partial Y} + \frac{1}{\text{Re}} \left(\frac{\partial^2 V}{\partial X^2} + \frac{\partial^2 V}{\partial Y^2} \right) \quad (3)$$

ω is angular velocity of the rotor. p : the pressure, Re : the Reynolds number based on the radius of the rotor and the uniform flow. Re is fixed to 10^5 in this study. (X, Y) and (U, V) are the position and velocity components in rotational coordinate system. (x, y) and (u, v) are those in stationary one. Equations (4)-(7) express relation between them. θ is rotation angle from rest as is shown in Fig.2.

$$X = x \cos \theta - y \sin \theta \quad (4)$$

$$Y = x \sin \theta + y \cos \theta \quad (5)$$

$$U = u \cos \theta - v \sin \theta - \omega Y \quad (6)$$

$$V = u \sin \theta + v \cos \theta + \omega X \quad (7)$$

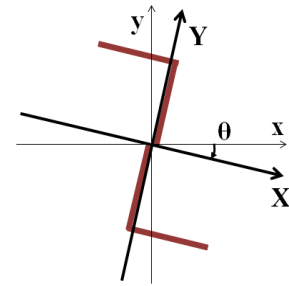


Fig. 2. Stationary and rotational coordinate systems.

3.2 Computational Method

Equations (1)-(3) are transformed by the fractional step method [3] so that the computer can calculate them. Pressure terms are separated into other equations as follows:

$$U^* = U^n + \Delta t \left\{ -U^n \frac{\partial U^n}{\partial X} - V^n \frac{\partial U^n}{\partial Y} + \omega^2 X - 2\omega V^n + \frac{1}{\text{Re}} \left(\frac{\partial^2 U^n}{\partial X^2} + \frac{\partial^2 U^n}{\partial Y^2} \right) \right\} \quad (8)$$

$$V^* = V^n + \Delta t \left\{ -U^n \frac{\partial V^n}{\partial X} - V^n \frac{\partial V^n}{\partial Y} + \omega^2 Y + 2\omega U^n + \frac{1}{\text{Re}} \left(\frac{\partial^2 V^n}{\partial X^2} + \frac{\partial^2 V^n}{\partial Y^2} \right) \right\} \quad (9)$$

$$\frac{\partial^2 p^{n+1}}{\partial X^2} + \frac{\partial^2 p^{n+1}}{\partial Y^2} = \frac{1}{\Delta t} \left(\frac{\partial^2 U^*}{\partial X^2} + \frac{\partial^2 V^*}{\partial Y^2} \right) \quad (10)$$

$$U^{n+1} = U^* - \Delta t \frac{\partial p^{n+1}}{\partial X} \quad (11)$$

$$V^{n+1} = V^* - \Delta t \frac{\partial p^{n+1}}{\partial Y} \quad (12)$$

(U^*, V^*) is the intermediate velocity. (U^n, V^n) is velocity components at time-step n . (U^{n+1}, V^{n+1}) and p^{n+1} are velocity components and pressure at time-step $n + 1$. Time development is carried out by using Eqs. (8)-(12).

All the spatial derivatives except nonlinear terms are approximated by the central differences. Nonlinear terms are approximated by the third order upwind difference. The third order upwind differences make it possible to calculate the flow at high Reynolds number even if the grids are not fine enough [4].

3.3 Motion of the Rotor

If the flow around the rotor was calculated, the pressure that pushes the blades of rotor can be obtained. It provides calculation for the force that rotates the rotor called "torque".

The difference of pressure applied to the inside and outside of the blade generates a force to push the blade of the rotor. The local surface Δx_w shown in Fig. 3 receive the torque ΔN .

$$\Delta N = \Delta x_w (p_{in} - p_{out}) r \quad (13)$$

When $p_{in} > p_{out}$ then $\Delta N > 0$, torque acts in the direction of rotation. On the other hand, When $p_{in} < p_{out}$, torque prevents the rotation of the rotor. The force of rotation, torque N is integral of the rotating-directional component of all local torque over the blade of the rotor ($\sin \varphi \Delta N$).

Equation of motion of a Savonius rotor is as follows:

$$I \frac{\partial \omega}{\partial t} = N - B \quad (14)$$

I is the moment of inertia, N : torque calculated from Eq. (13), B : friction from rotation axis. B is proportional to ω . Differential equation (14) is calculated by Runge-Kutta method. When ω is obtained, rotate the Savonius rotor accordingly.

3.4 Computational Region and Conditions

Equations (8)-(14) are solved on the grid points as is shown in Fig. 4. The grid is fixed on the blade of the rotor. When the rotor rotates, the grid rotates with it.

A uniform flow is assumed on external side of computer region. No-slip condition is employed on the blade of the rotor. This means fluid on the blade rotate with blade at same speed. The other boundary conditions are shown in Table 1.

ω is set 0 as initial condition. It means the rotor is in a stationary state at first. The force of the wind will increase ω as the calculation progresses.

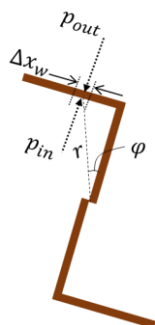


Fig. 3. Torque on a local surface.

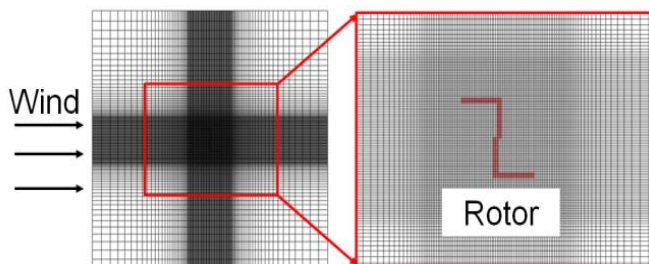


Fig. 4. Computational grid.

Table 1. Boundary conditions

	External side of computer region	On the blade of the rotor
Velocity	Uniform flow $u = 1.0, v = 0.0$	No-slip condition on the rotational coordinate $U = 0.0, V = 0.0$
Pressure	$\frac{\partial p}{\partial x} = \frac{\partial p}{\partial y} = 0$	Arithmetic average of pressure on the neighborhood grid points in fluid

4. Results

Figures 5 and 6 are the visualized flow field around rotating Savonius rotor. Color shows the non-dimensional pressure field. Blue means the lowest pressure in the field at that moment. Red means the highest. Vector show the velocity field of the flow.

Figures 7 and 8 show simplified schematic views of Figs. 5 and 6 respectively. In Figs. 5 and 7, the wind enters the upper blade and pushes the blade clockwise. It concludes $p_{in} > p_{out}$ in Eq. (13) in most local surface. Torque N becomes positive, and it acts in the direction of rotating the rotor. In Figs. 6 and 8, the wind is difficult to enter the upper blade. Wind would rather push the lower blade counterclockwise. Furthermore, the low pressure field on the leeward side of lower blade suck down and rotate the blade counterclockwise. It concludes $p_{in} < p_{out}$ in Eq. (13) in most local surface. Torque N becomes negative, and the rotor seeks to rotate counterclockwise.

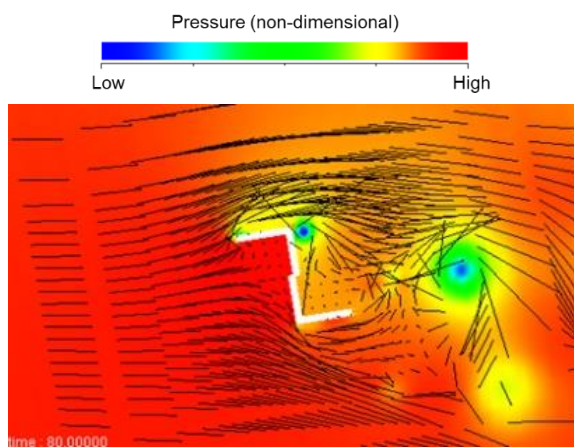


Fig. 5. Flow field which rotates the rotor fast.

Wind push the blade to clockwise

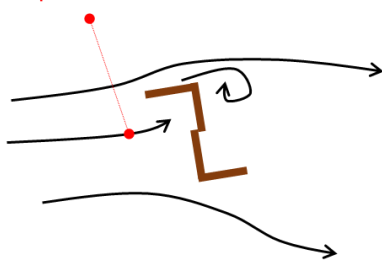


Fig. 7. Schematic view of Fig. 5

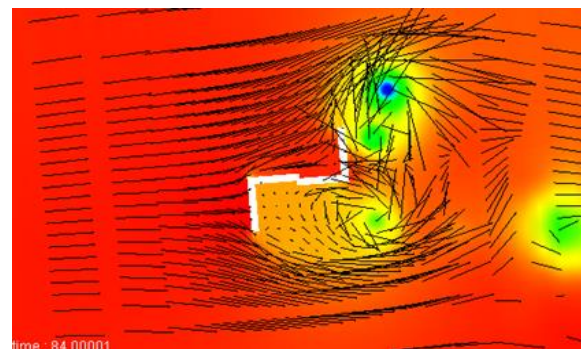


Fig. 6. Flow field which cannot rotates the rotor.

Wind push to counterclockwise

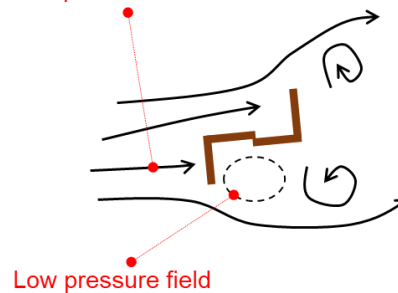


Fig. 8. Schematic view of Fig. 6

The time variation of the torque N is shown in Fig. 9. As already stated, the rotor angle as is shown in Figs. 5 and 7 generate large torque. It in Figs. 6 and 8 generates small or negative torque. The reason for periodically vibrating of torque N is the point-symmetric shape of the rotor.

The time variation of the angular velocity ω of the rotor calculated by Eq. (14) is shown in Fig. 10. The rotor in a stationary state starts rotating by the force of the wind. Then it rotates at speed within a certain range. Large torque N starts to rotate the rotor quickly, in other words, ω become large. Negative torque N stops the rotor, then ω become small. ω vibrates a little late as the increase and decrease of torque N is periodically repeated.

The rotor rotates by force of the wind, instead of rotating at a constant angular velocity. It permits to simulate under more realistic conditions.

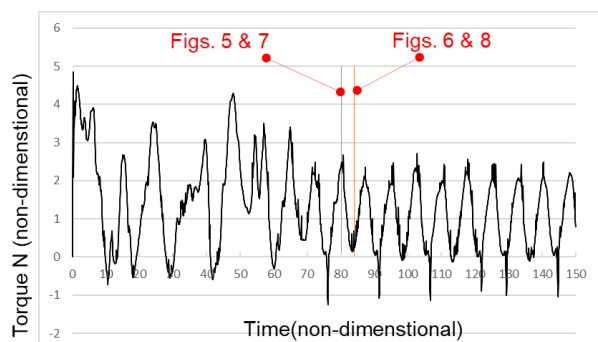


Fig. 9. The time variation of the torque.

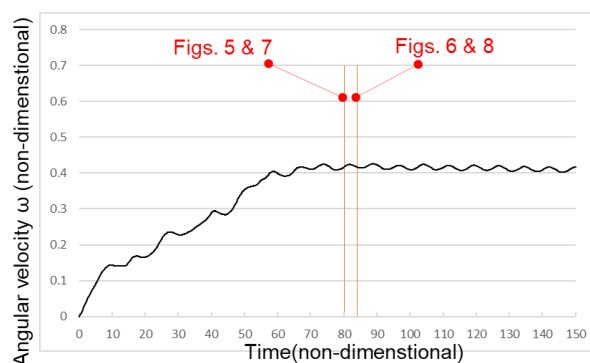


Fig. 10 The time variation of the angular velocity.

5. Other Possibilities

More than one wind turbines often installed densely. It is necessary to consider the influence of the flow created by one wind turbine on other wind turbines. Since each wind turbine rotates independently, it is difficult to make a grid. Overset grid shown in Fig. 11 will be employed.

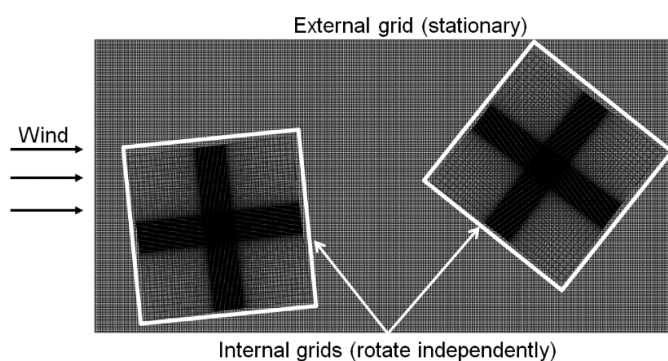


Fig. 11. Conceptual drawing of overset grid for simulation of multiple wind turbines.

In order to make an efficient wind turbine, it is necessary to decide the optimum blade shape, the arrangement of the wind turbine. Too many parameters have to be decided in the process. For example, the thickness and length of the blade, the shape of the tip of the blade, the position and distance of the wind turbine, etc. It is impossible to experiment with all parameter combination. Simulation has the potential to find the optimal solution automatically.

6. Conclusion

Simulation technology and the possibility of its application to green environment were discussed in this paper. Savonius rotor was introduced as one example. The unsteady rotation of the rotor could be carried out. Simulation of interaction between more than one wind turbines is a future work.

References

- [1] S.J.Savonius, "The S-rotor and its applications" *Mech Eng.* Vol. 53, No. 5, pp. 333-337, 1931.
- [2] I. Ushiyama, H. Nagai and J. Shinoda, "Experimentally Determining the Optimum Design Configuration for Savonius Rotors", *Bulletin of JSME*, Vol. 29, No. 258, 1986.
- [3] N.N. Yanenko, "The method of fractional steps", *Springer-Verlag*, 1971.
- [4] T.Kawamura and K. Kuwahara, "Computation of high Reynolds number flow around a circular cylinder with surface roughness", *AIAA Paper*, 84-0340, 1984.